Nonisothermal Crystallization Kinetics of Polyoxymethylene/Montmorillonite Nanocomposite

W. XU,[1,2] M. GE,[2] P. HE[1]

[1] Department of Polymer Science and Engineering, University of Science and Technology of China, Hefei 230026, Anhui, China

[2] College of Chemical Engineering, Hefei University of Technology, Hefei 230009, Anhui, China

Received 11 December 2000; accepted 7 March 2001

ABSTRACT: The nonisothermal crystallization kinetics of polyoxymethylene (POM), polyoxymethylene/Na–montmorillonite (POM/Na–MMT), and polyoxymethylene/organic–montmorillonite (POM/organ–MMT) nanocomposites were investigated by differential scanning calorimetry at various cooling rates. The Avrami analysis modified by Jeziorny and a method developed by Mo were employed to describe the nonisothermal crystallization process of POM/Na–MMT and POM/organ–MMT nanocomposites. The difference in the values of the exponent n between POM and POM/montmorillonite nanocomposites suggests that the nonisothermal crystallization of POM/Na–MMT and POM/organ–MMT nanocomposites corresponds to a tridimensional growth with heterogeneous nucleation. The values of half-time and the parameter Z_c, which characterizes the kinetics of nonisothermal crystallization, show that the crystallization rate of either POM/Na–MMT or POM/organ–MMT nanocomposite is faster than that of virgin POM at a given cooling rate. The activation energies were evaluated by the Kissinger method and were 387.0, 330.3, and 328.6 kJ/mol for the nonisothermal crystallization of POM, POM/Na–MMT nanocomposite, and POM/organ–MMT nanocomposite, respectively. POM/montmorillonite nanocomposite can be as easily fabricated as the original polyoxymethylene, considering that the addition of montmorillonite, either Na–montmorillonite or organ–montmorillonite, may accelerate the overall nonisothermal crystallization process. © 2001 John Wiley & Sons, Inc. J Appl Polym Sci 82: 2281–2289, 2001

Key words: polyoxymethylene; montmorillonite; nanocomposite; nonisothermal crystallization kinetics

INTRODUCTION

The physical and mechanical properties of the hybrid organic–inorganic composites are greatly influenced by the length scale of the component phase.[1–3] Intercalation of mica-type layered silicates proved to be a versatile approach to polymer–clay nanocomposites.[4–9] These nanocomposites exhibit higher modulus, less thermal expansion coefficient and gas permeability, increased swelling resistance, and enhanced ionic conductivity compared to the properties of pure polymer. The enhanced properties are presumably attributable to the nanoscale structure of the hybrids and the synergism between the polymer and the silicate. The silicate used is usually montmorillonite, a smectic clay. Many approaches have been employed to prepare polymer–clay nanocomposites. In most cases,

Correspondence to: P. He (hpsm@ustc.edu.cn).

Contract grant sponsor: Nature Science Foundation (Anhui Province, China).

Journal of Applied Polymer Science, Vol. 82, 2281–2289 (2001)

© 2001 John Wiley & Sons, Inc.

the process involves intercalation of a suitable monomer and exfoliation of the layered galleries into their nanoscale elements by subsequent polymerization. Pinnavaia[10–12] prepared monolithic epoxy–exfoliated-clay nanocomposites from the reaction of alkylammonium-exchanged smectite clays with diglycidyl ether of bisphenol A and *m*-phenylenediamine as the curing agent. The reinforcement provided by the silicate layers at 16 wt % loading was manifested by a greater than 10-fold improvement in both tensile strength and modulus. Lee[13] synthesized PS–clay nanocomposite by using emulsion polymerization. However, for many industrial polymers, for example, polystyrene,[6,14] polyamide,[15] and poly(ethylene oxide),[16] one promising approach to prepare the nanocomposites is to intercalate the melt polymer directly.

Of considerable importance is how the layered silicate existing in the intercalated polymer affects the crystallization procedure. For the polymer crystallization, generally, studies of crystallization process are limited to isothermal conditions,[17] the theoretical analysis is easy to handle, and problems associated with cooling rates and thermal gradients within the specimens are avoided. In practice, however, the crystallization in a continuously changing thermal environment is of greater interest, given that industrial processes generally proceed under nonisothermal conditions.

In this contribution, the polyoxymethylene/montmorillonite (POM/MMT) intercalated nanocomposite was prepared by direct-melt intercalation, and several nonisothermal crystallization kinetic equations were employed to study the crystallization characteristics of POM/MMT nanocomposites. Dynamic DSC thermograms supplied the necessary data. By using an evaluation method proposed by Kissinger, activation energies were estimated for the crystallization of POM/MMT nanocomposites.

EXPERIMENTAL

Materials

Polyoxymethylene (POM, 500P) used was purchased from Dupont (Wilmington, DE). Na^+–montmorillonite (Na–MMT), with a cation exchange capacity (CEC) value of 100 mmol/100 g, was kindly provided by Qingshan Chemistry Agent Factory (Lin'an, China). $CH_3(CH_2)_{15}N(CH_3)_3Br$, the surfactant of clay, was purchased from the Research Institute of Xinhua, Active Material (Changzhou, China).

Preparation of Polyoxymethylene/Montmorillonite Nanocomposite

According to our previous study,[18] organically modified montmorillonite (organ–MMT) was prepared by a cation-exchange reaction between Na^+–MMT and $CH_3(CH_2)_{15}N(CH_3)_3Br$. Melt intercalation were carried out by blending the montmorillonite powders (Na–MMT or org–MMT) and POM (5 : 95, by weight) and melt mixing the admixture in a roller mill at the temperature of 175–180°C for 10 min. Upon completion of mixing, the molten polymer was removed and allowed to cool. The mixture was then compression molded, at 180°C for 30 min, to give a 3-mm-thick sheet.

X-ray Diffraction Analysis

The lattice spacing of montmorillonite was monitored on the Rigaku-D/max-γB rotating anode X-ray diffractometer (Rigaku, Japan) using a graphite monochrometer with a 40-kV tube voltage and a 100-mA tube current. The scanning range was 2.2–10° with a scanning rate of 2°/min and the CuK_α line (λ = 0.15418 nm) was used.

Nonisothermal DSC Analysis

A Perkin–Elmer DSC 2C apparatus (Perkin Elmer Cetus Instruments, Norwalk, CT) was used for measuring nonisothermal crystallization kinetics in the cooling mode from the molten state (melt crystallization). The temperature and energy readings were calibrated with indium at each cooling rate employed in the measurements. All measurements were carried out in a nitrogen atmosphere. For nonisothermal melt crystallization, the raw sample was heated to 190°C and kept for 5 min in the DSC cell to destroy any nuclei that might act as seed crystals. The sample was cooled at constant rates of 5, 10, 20, and 40 K/min, respectively. The exothermic crystallization peak was recorded as a function of temperature.

RESULTS AND DISCUSSION

X-ray Diffraction Analysis

XRD patterns, responding to the change in basal spacing of montmorillonite, are shown in Figure 1

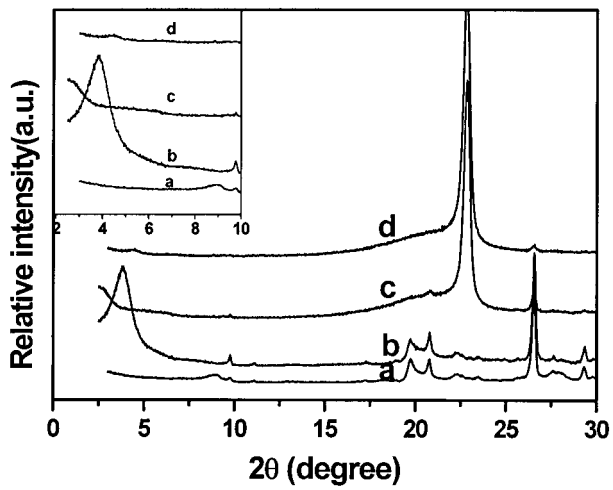

Figure 1 X-ray diffraction patterns: (a) Na–MMT; (b) organ–MMT; (c) POM/organ–MMT; (d) POM/Na–MMT.

for Na–MMT, organ–MMT, POM/Na–MMT, and POM/organ–MMT nanocomposites. For the organ–MMT, it is noteworthy that the (001) peak with d_{001} = 2.31 nm shifted to a lower angle (2θ = 3.82°), comparable to that of the Na–MMT. For the POM/Na–MMT composite, the (001) diffraction peak with d_{001} = 1.92 nm appeared at 2θ = 4.60°. Compared to the Na–MMT composite's d_{001} of 0.99 nm, the lattice spacing increased by 0.93 nm during the procedure of direct melt mixing between POM and Na–MMT, indicating that the intercalated POM occupied an interlayer space of only 0.93 nm. This may be the result of the strong interaction between POM molecules and the silicate layer. POM molecules can penetrate the silicate particle and be intercalated into the interlayer of montmorillonite. Giannelis[16] prepared the poly(ethylene oxide)/Li–montmorillonite intercalated nanocomposite by direct intercalation, which showed an ordered multilayer structure with a repeat unit of 1.77 nm. However, for the POM/organ–MMT composite, the diffraction peak appeared at 2θ = 2.5° with d_{001} of 3.52 nm. Compared to d_{001} of 0.99 nm for Na–MMT, the lattice spacing of montmorillonite increased by 2.53 nm during the procedure of direct melt mixing between POM and organ–MMT. Thus, the POM/Na–MMT and POM/organ–MMT intercalated nanocomposites were obtained with the lattice spacings of 1.92 and 3.52 nm, respectively. The d_{001} of POM/organ–MMT nanocomposite is larger than that of POM/Na–MMT, indicating that the POM molecular chain can be easily intercalated into the silicate interlayer of org–MMT.

Crystallization Behavior of POM/MMT Nanocomposite

The crystallization exotherms of pristine POM and both POM/Na–MMT and POM/organ–MMT nanocomposites at various cooling rates are presented in Figure 2. From these curves, some useful data can be obtained for describing their nonisothermal crystallization behavior, such as the peak temperature (T_p), at which POM has the fastest crystallization, and relative degree of crystallinity (X_t) as a function of crystallization temperature. First, it is clearly seen from Figure 2 that T_p shifts, as expected, to a lower temperature when the cooling rate increases, which is attributed to the lower time scale that allows the polymer to crystallize as the cooling rate increases, therefore requiring a higher undercooling to initiate crystallization. On the other hand, when the specimens are cooled fast, the motion of POM molecules is not able to follow the cooling temperature. Second, for a given cooling rate, the POM/organ–MMT nanocomposite's T_p is almost equal to that of the POM/Na–MMT nanocomposite, but higher than that of pure POM, as shown in Table I. This means that the addition of montmorillonite (either Na–MMT or organ–MMT) into POM increases the crystallization rate of POM, indicating that the montmorillonite layer easily absorbs the POM molecular segments, and this absorption leads to the occurrence of crystallization of POM molecules at higher temperatures. For the nonisothermal crystallization of POM and both POM/Na–MMT and POM/organ–MMT nanocomposites, the crystallization enthalpies (ΔH_c) have the same variation tendency as the cooling rate increases.

Nonisothermal Crystallization Kinetics of POM/MMT Nanocomposite

The relative degree of crystallinity X_t, as a function of crystallization temperature T, is defined as

$$X_t = \int_{T_0}^{T} (dH_c/dT)\, dT \Big/ \int_{T_0}^{T_\infty} (dH_c/dT)\, dT \tag{1}$$

where T_0 and T_∞ are the onset and end of crystallization temperatures, respectively.

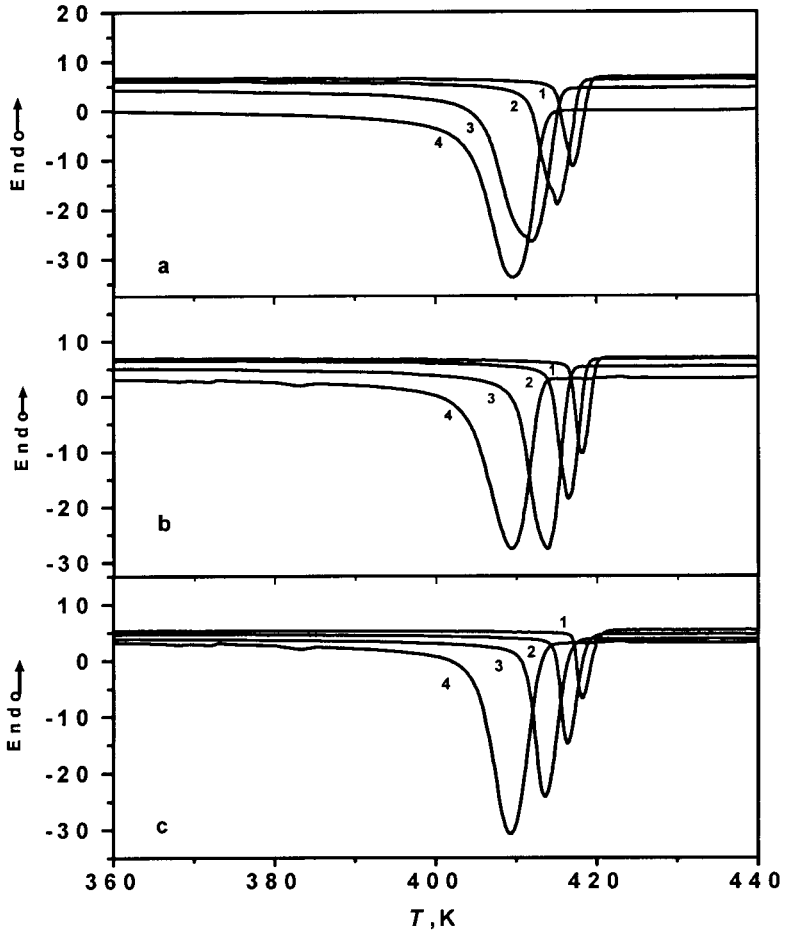

Figure 2 DSC thermograms of (a) POM, (b) POM/Na–MMT nanocomposite, and (c) POM/organ–MMT nanocomposite at various cooling rates: 1–5 K/min, 2–10 K/min, 3–20 K/min, 4–40 K/min.

Figure 3 shows the relative degree of crystallinity as a function of temperature for POM/Na–MMT and POM/organ–MMT nanocomposites at different cooling rates. It can be seen that all these curves have the same sigmoidal shape. Using the equation $t = (T_0 - T)/\Phi$ (where T is the temperature at crystallization time t, and Φ is the cooling rate), the horizontal temperature axis of Figure 3 could be changed into a time scale (see Fig. 4). It can be seen that the higher the cooling rate, the shorter the time for completing the crystallization. The half-time ($t_{1/2}$) of nonisothermal crystallization of POM/Na–MMT and POM/organ–MMT nanocomposites could be obtained from Figure 4, and the results are listed in Table I. It can be seen that, as expected, the order of $t_{1/2}$ decreases with the increasing cooling rates for POM/Na–MMT and POM/organ–MMT nanocomposites. However, at a given cooling rate, the $t_{1/2}$ value of the POM/organ–MMT nanocomposite is lower than that of the POM/Na–MMT nanocomposite, signifying the difference of accelerating the overall crystallization process with the addition of organ–MMT or Na–MMT. A reasonable explanation is that the lattice spacing of organ–MMT is larger than that of Na–MMT, and a stronger interaction exists between the POM molecule and the silicate layer, leading to a greater nucleation effect of organ–MMT than that of Na–MMT.

The approach adopted here was to use the Avrami equation,[19]

$$1 - X_t = \exp(-Z_t t^n) \tag{2}$$

where the exponent n is a mechanism constant, which is dependent on the type of nucleation and

Table I Parameters of Sample During Nonisothermal Crystallization Process

Sample	Φ (K/min)	Z_c	n	$t_{1/2}$	T_p (K)	ΔH_c (J/g)
POM	5	1.09	4.7	0.78	417.07	134.39
	10	1.27	3.9	0.52	415.16	135.15
	20	1.18	3.3	0.31	411.98	142.79
	40	1.14	3.2	0.15	409.57	101.26
POM/Na–MMT nanocomposite	5	1.44	5.3	0.72	418.22	120.36
	10	1.45	4.2	0.46	416.45	125.73
	20	1.27	4.2	0.29	413.86	127.92
	40	1.17	3.6	0.20	409.37	118.37
POM/organ–MMT nanocomposite	5	1.15	4.8	0.54	418.24	121.26
	10	1.39	4.6	0.41	416.33	125.73
	20	1.28	4.1	0.27	413.56	134.65
	40	1.19	4.5	0.16	409.28	116.06

growth process parameters, and the parameter Z_t is a composite rate constant that involves both nucleation and growth rate parameters. Using eq. (2) in double-logarithmic form,

$$\ln[-\ln(1 - X_t)] = \ln Z_t + n \ln t \qquad (3)$$

and plotting $\ln[-\ln(1 - X_t)]$ against $\ln t$ for each cooling rate, a straight line is obtained (data at low degree of crystallinity were only used in the linear regression; see Fig. 5); thus two adjustable parameters, Z_t and n, can be obtained. It must be taken into account that in nonisothermal crystallization, the Z_t and n parameters do not have the same physical meaning as in the isothermal crystallization because the temperature changes constantly in nonisothermal crystallization. This affects the rates of both nuclei formation and

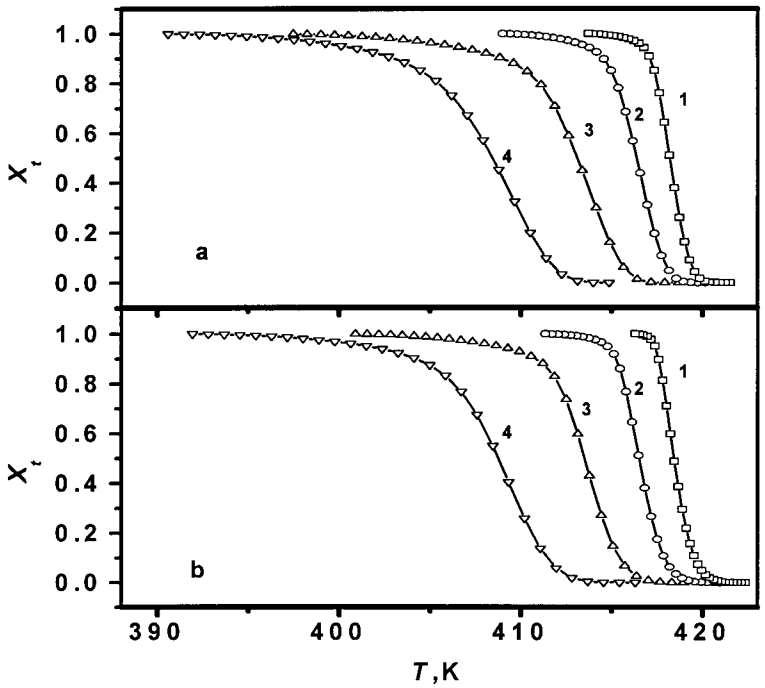

Figure 3 Plots of X_t versus T for crystallization of (a) POM/Na–MMT nanocomposite and (b) POM/organ–MMT nanocomposite at various cooling rates: 1–5 K/min, 2–10 K/min, 3–20 K/min, 4–40 K/min.

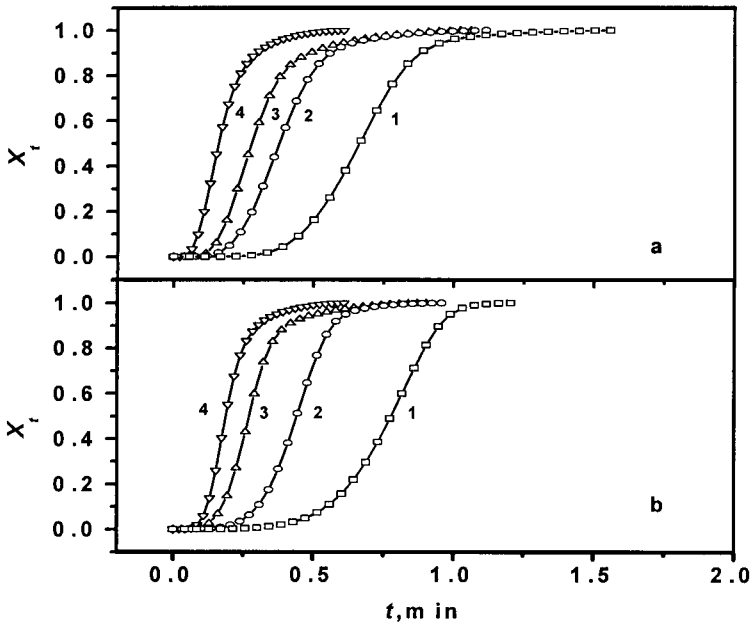

Figure 4 Plots of X_t versus t for crystallization of (a) POM/Na–MMT nanocomposite and (b) POM/organ–MMT nanocomposite at various cooling rates: 1–5 K/min, 2–10 K/min, 3–20 K/min, 4–40 K/min.

spherulite growth ascribed to their temperature dependence. In this case, Z_t and n are two adjustable parameters to be fit to the data only. Although the physical meaning of Z_t and n cannot be related to the nonisothermal case in a simple way, the use of eq. (2) provides further insight into the kinetics of nonisothermal crystallization.

Considering the nonisothermal character of the process investigated, Jeziorny[20] presented the final form of the parameter characterizing the kinetics of nonisothermal crystallization as follows:

$$\ln Z_c = \ln Z_t/\Phi \tag{4}$$

The results, obtained from Avrami plots and the Jeziorny method, are also listed in Table I. The exponent n varied from 3.2 to 4.7 for POM, from 3.5 to 5.3 for the POM/Na–MMT nanocomposite, and from 4.0 to 4.8 for the POM/organ–MMT nanocomposite. There was some confusion of Avrami exponent values of virgin POM in the literature, which is attributed to the complication of POM crystallization. For example, Plummer[21] obtained a value of 2 and Phillips[22] reported a value of 3–4. Although the exponent n obtained from nonisothermal crystallization showed a wide range of values and more scattered than those obtained from isothermal crystallization,[23] it is interesting that the values of n for POM/Na–MMT and POM/organ–MMT nanocomposites are larger than that of virgin POM at the same cooling rate, indicating that the montmorillonite acts as a nucleating agent for the POM matrix. The same conclusion is reasonable for polypropylene (PP)[24] and for POM with nucleating agents (of both attapulgite and diatomite) in isothermal crystallization.[17] The Z_c values of POM/Na–MMT and POM/organ–MMT nanocomposites are, as expected, higher than that of virgin POM at same cooling rate.

Ozawa[25] extended the Avrami equation to the nonisothermal condition. Assuming that the nonisothermal crystallization process may be composed of infinitesimally small isothermal crystallization steps, the following equation was derived:

$$1 - X_t = \exp[-K(T)/\Phi^m] \tag{5}$$

where $K(T)$ is the cooling rate function; Φ is the cooling rate; and m is the Ozawa exponent, which is dependent on the dimension of the crystal growth. Taking the double-logarithmic form,

$$\ln[-\ln(1 - X_t)] = \ln K(T) - m \ln \Phi \tag{6}$$

and plotting $\ln[-\ln(1 - X_t)]$ against $\ln \Phi$ at a given temperature, a straight line should be ob-

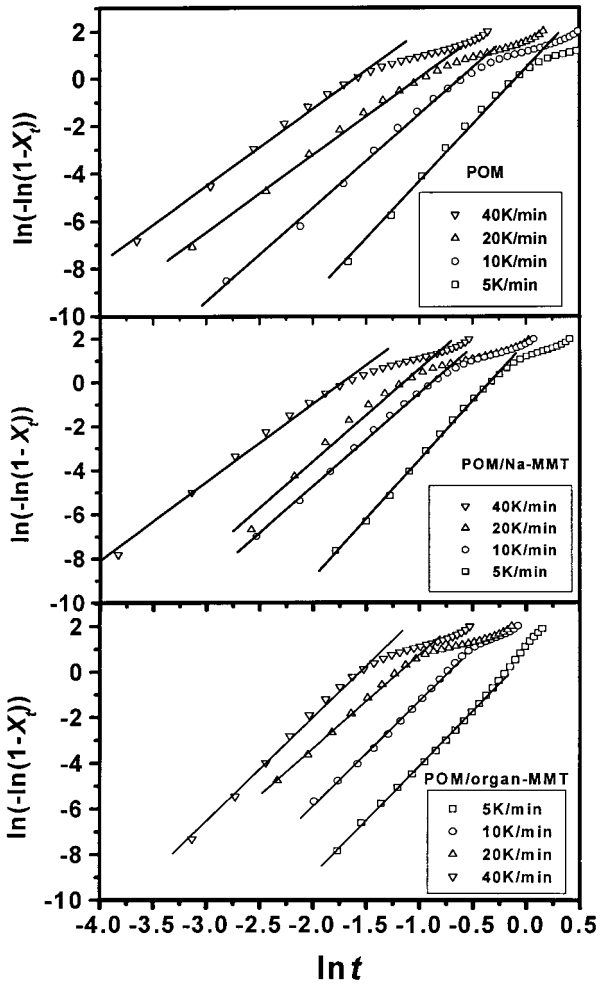

Figure 5 Plots of $\ln[-\ln(1 - X_t)]$ versus $\ln t$ for crystallization of POM and both POM/Na–MMT and POM/organ–MMT nanocomposites.

tained if the Ozawa method is valid. Thus $K(T)$ and m can be determined from the intercept and slope, respectively.

Figure 6 shows the results for POM/Na–MMT and POM/organ–MMT nanocomposites according to Ozawa's method. The curvature in Figure 6 prevents an accurate analysis of the nonisothermal crystallization data. This can be explained that, at a given temperature, the crystallization processes at different cooling rates are at different stages, that is, the lower cooling rate process is toward the end of the crystallization process, whereas at the higher cooling rate, the crystallization process is at an early stage. Although Ozawa's approach has been used to describe the nonisothermal crystallization behavior of polypropylene with nucleating agent DBS,[26] the change in the slope with temperature [Fig. 6(a) and (b)] means that the parameter m is not a constant during crystallization, indicating that Ozawa's approach is not a good method to describe the nonisothermal crystallization process of POM/Na–MMT and POM/organ–MMT nanocomposites.

A method developed by Mo[27] was also employed to describe the nonisothermal crystallization for comparison. For the nonisothermal crystallization process, physical variables relating to the process are the relative degree of crystallinity X_t, cooling rate Φ, and crystallization temperature T. Both the Ozawa and Avrami equations can relate these variables as follows:

$$\ln Z_t + n \ln t = \ln K(T) - m \ln \Phi \tag{7}$$

and by rearrangement

$$\ln \Phi = \ln F(T) - a \ln t \tag{8}$$

where $F(T) = [K(T)/Z_t]^{1/m}$ refers to the cooling rate value, which must be chosen within unit crystallization time when the measured system amounts to a certain degree of crystallinity; a is the ratio of the Avrami exponent n to the Ozawa

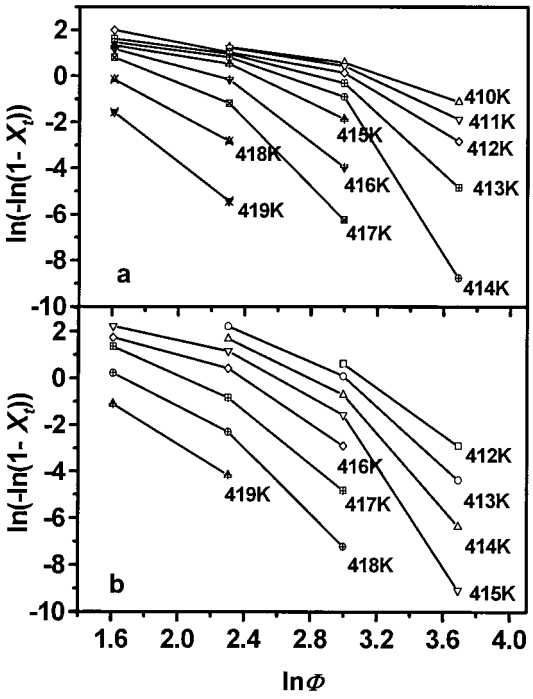

Figure 6 Ozawa plots of $\ln[-\ln(1 - X_t)]$ versus $\ln \Phi$ for crystallization of (a) POM/Na–MMT nanocomposite and (b) POM/organ–MMT nanocomposite.

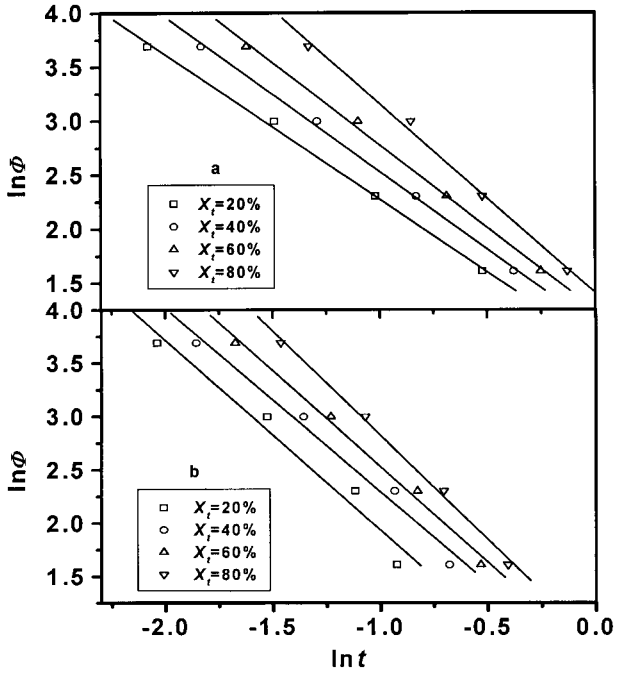

Figure 7 Plots of ln Φ versus ln t for (a) POM/Na–MMT nanocomposite and (b) POM/organ–MMT nanocomposite.

exponent m ($a = n/m$). According to eq. (8), at a given degree of crystallinity, plotting ln Φ versus ln t (Fig. 7) yields a linear relationship between ln Φ and ln t. The data of kinetic parameter $F(T)$ and a estimated from the intercept and slope for POM/Na–MMT and POM/organ–MMT nanocomposites are listed in Table II. It can be seen from Table II

Table II Nonisothermal Crystallization Kinetic Parameters at Different Degrees of Crystallinity

Sample	X_t (%)	$F(T)$	a	ΔE (kJ/mol)
POM	20	3.63	1.28	
	40	4.67	1.29	
	60	5.54	1.40	387.0
	80	7.56	1.45	
POM/Na–MMT nanocomposite	20	2.53	1.34	
	40	2.97	1.43	
	60	3.48	1.53	330.3
	80	4.08	1.75	
POM/organ–MMT nanocomposite	20	1.17	1.75	
	40	1.78	1.81	
	60	2.08	1.91	328.6
	80	2.38	1.98	

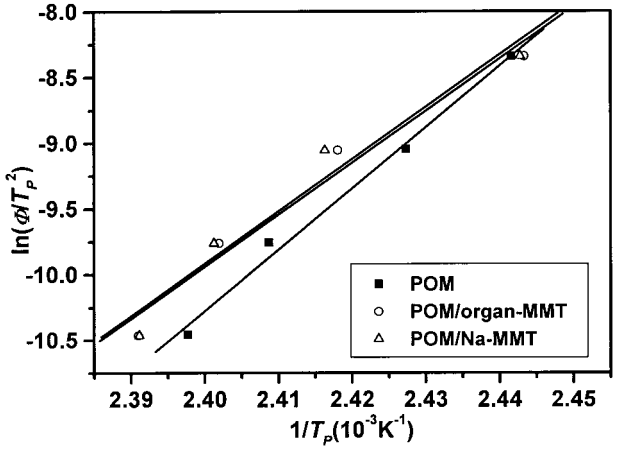

Figure 8 Plots of ln(Φ/T_p^2) versus $1/T_p$ for POM and both POM/Na–MMT and POM/organ–MMT nanocomposites.

that $F(T)$ systematically increases with the increase in the relative degree of crystallinity for virgin POM and both POM/Na–MMT and POM/organ–MMT nanocomposites. The value of a varies from 1.28 to 1.45 for POM, from 1.34 to 1.75 for the POM/Na–MMT nanocomposite, and from 1.75 to 1.98 for the POM/organ–MMT nanocomposite. It is clear that this approach is successful in describing the nonisothermal process of virgin POM and both POM/Na–MMT and POM/org–MMT nanocomposites as the same as that of PEEK[27] and PHB–PVAc blends.[28]

In addition, the method often used for evaluation of activation energy at different cooling rates was proposed by Kissinger,[29] based on the following equation:

$$\frac{d[\ln(\Phi/T_p^2)]}{d(1/T_p)} = -\frac{\Delta E}{R} \tag{9}$$

where R is the universal gas constant and ΔE is the activation energy for crystallization. From the slope of the plot $\ln(\Phi/T_p^2) \approx 1/T_p$ (Fig. 8), activation energies of nonisothermal melt crystallization of virgin POM, POM/Na–MMT nanocomposite, and POM/organ–MMT nanocomposite were determined to be 387.0, 330.3, and 328.6 kJ/mol, respectively. It can be seen that the activation energy of nonisothermal crystallization of either POM/Na–MMT nanocomposite or POM/organ–MMT nanocomposite is lower than that of virgin POM. Accordingly, the addition of montmorillonite, Na–montmorillonite, or organ–montmorillonite may accelerate the overall nonisothermal

crystallization process of POM. The POM/MMT nanocomposite, as original polyoxymethylene, can be easily fabricated (for instance, by injection molding) without any additional requirements.

CONCLUSIONS

POM/Na–MMT and POM/organ–MMT nanocomposites were prepared by melt intercalation. The Ozawa analysis failed to provide an adequate description of the nonisothermal crystallization of POM/Na–MMT and POM/organ–MMT nanocomposites because of the comparisons of different stages of crystallization at different cooling rates. The Avrami analysis modified by Jeziorny and a method developed by Mo were successful in describing the nonisothermal crystallization process of virgin POM and both POM/Na–MMT and POM/organ–MMT nanocomposites. The difference in the values of the exponent n between virgin POM and POM/MMT nanocomposite, either POM/Na–MMT or POM/organ–MMT nanocomposite, suggested that the nonisothermal crystallization of POM/MMT nanocomposite corresponds to a tridimensional growth with heterogeneous nucleation. The values of half-time and the parameter Z_c, which characterizes the kinetics of nonisothermal crystallization, showed that the crystallization rate of either POM/Na–MMT or POM/organ–MMT nanocomposite is faster than that of POM at a given cooling rate, and the crystallization rate of POM/organ–MMT nanocomposite is faster than that of POM/Na–MMT nanocomposite because of the alkylammonium-exchanged treatment for Na–montmorillonite. The activation energies were evaluated by the Kissinger method to be 387.0, 330.3, and 328.6 kJ/mol for the nonisothermal crystallization of POM, POM/Na–MMT nanocomposite, and POM/organ–MMT nanocomposite, respectively. The addition of montmorillonite, either Na–montmorillonite or organ–montmorillonite, may accelerate the overall nonisothermal crystallization process of POM, and the POM/MMT nanocomposite can be easily fabricated the same as the original polyoxymethylene without any additional requirements.

The authors gratefully acknowledge the financial support from the Nature Science Foundation of Anhui Province, China.

REFERENCES

1. Whiteside, G. M.; Mathias, T. P.; Seto, C. T. Science 1991, 254, 1312.
2. Gleiter, H. Adv Mater (Weinheim, Ger) 1992, 4, 474.
3. Novak, B. Adv Mater (Weinheim, Ger) 1993, 5, 422.
4. Vaia, R. A.; Giannelis, E. P. Macromolecules 1997, 30, 8000.
5. Vaia, R. A.; Vasudevan, S.; Krawiec, W.; Giannelis, E. P. Adv Mater (Weinheim, Ger) 7, 154, 1995.
6. Vaia, R. A.; Ishii, H.; Giannelis, E. P. Chem Mater 1995, 5, 1694.
7. Messersmith, P. B.; Giannelis, E. P. Chem Mater 1994, 6, 1719.
8. Kojima, Y.; Usuki, A.; Kawasumi, M. J Mater Res 1993, 8, 1185.
9. Aranda, P.; Ruiz–Hitzky, E. Chem Mater 1992, 4, 1395.
10. Lan, T.; Kaviratna, P. D.; Pinnavaia, T. J. Chem Mater 1995, 7, 2144.
11. Lan, T.; Pinnavaia, T. J. Chem Mater 1994, 6, 2216.
12. Lan, T.; Kaviratna, P. D.; Pinnavaia, T. J. Polym Mater Sci Eng 1994, 71, 527.
13. Noh, M. W.; Lee, D. C. Polym Bull 1999, 42, 619.
14. Sikka, M.; Cerini, L. N.; Ghosh, S. S.; Winey, K. I. J Polym Sci Part B Polym Phys 1996, 34, 1443.
15. Liu, L.; Qi, Z.; Zhu, X. J Appl Polym Sci 1999, 71, 1133.
16. Vaia, R. A.; Sauer, B. B.; Tse, O. K.; Giannelis, E. P. J Polym Sci Part B Polym Phys 1997, 35, 59.
17. Weibing, X. U.; Pingsheng, H. E. J Appl Polym Sci 2001, 80, 304.
18. Xu, W.; Ge, M.; He, P. China Plast 2000, 14, 28.
19. Ziakicki, A. Colloid Polym Sci 1974, 252, 433.
20. Jeziorny, A. Polymer 1978, 19, 1142.
21. Plummer, C. J. G.; Kausch, H. H. Colloid Polym Sci 1995, 273, 227.
22. Phillips, R.; Manson, J.-A. E. J Polym Sci Part B Polym Phys 1997, 35, 875.
23. Srinivas, S.; Babu, J. R.; Riffle, J. S.; Wilkes, G. L. Polym Eng Sci 1997, 37, 497.
24. Lim, G. B. A.; Lloyd, D. R. Polym Eng Sci 1993, 33, 513.
25. Ozawa, T. Polymer 1971, 12, 150.
26. Feng, Y.; Jin, X.; Hay, J. N. J Appl Polym Sci 1998, 69, 2089.
27. Liu, T. X.; Mo, Z. S.; Wang, S. E.; Zhang, H. F. Polym Eng Sci 1997, 37, 568.
28. An, Y.; Li, L.; Mo, Z. S.; Feng, Z. L. J Polym Sci Part B Polym Phys 1999, 37, 443.
29. Kissinger, H. E. J Res Natl Bur Stand (US) 1956, 57, 217.